

Superconductivity and fluctuating magnetism in quasi-two-dimensional κ -(BEDT-TTF)₂Cu[N(CN)₂]Br probed with implanted muons

T. Lancaster,^{1,*} S. J. Blundell,¹ F. L. Pratt,² and J. A. Schlueter³¹*Oxford University Department of Physics, Clarendon Laboratory, Parks Road, Oxford, OX1 3PU, United Kingdom*²*ISIS Facility, Rutherford Appleton Laboratory, Chilton, Oxfordshire, OX11 0QX, United Kingdom*³*Materials Science Division, Argonne National Laboratory, 9700 South Cass Avenue, Argonne, Illinois 60439, USA*

(Received 1 July 2010; revised manuscript received 8 November 2010; published 19 January 2011)

A muon-spin relaxation (μ^+ SR) investigation is presented for the molecular superconductor κ -(BEDT-TTF)₂Cu[N(CN)₂]Br. Evidence is found for low-temperature phase separation throughout the bulk of the material, with only a fraction of the sample showing a superconducting signal, even for slow cooling. Rapid cooling reduces the superconducting fraction still further. For the superconducting phase, the in-plane penetration depth is measured to be $\lambda_{\parallel} = 0.47(1) \mu\text{m}$, and evidence is seen for a vortex decoupling transition in applied fields above 40 mT. The magnetic fluctuations in the normal state produce a precipitous drop in relaxation rate above 100 K, and we discuss the possible causes for the unusual relaxation that we observe for $T > T_c$.

DOI: [10.1103/PhysRevB.83.024504](https://doi.org/10.1103/PhysRevB.83.024504)

PACS number(s): 74.70.Kn, 76.75.+i, 74.25.Ha

I. INTRODUCTION

The quasi-two-dimensional molecular series κ -(BEDT-TTF)₂X exemplifies the complex interplay of collective phenomena that occur in correlated electron systems.^{1,2} In particular, the proximity of superconducting κ -(BEDT-TTF)₂Cu[N(CN)₂]Br to a Mott transition, along with possible pseudogap physics and molecular disorder effects, has led to this material being extensively studied in recent years.³⁻⁷ Despite this intense interest, several experimental observations in this system lack a conclusive explanation,² and more experimental study is warranted. In this paper, we present a muon-spin relaxation (μ^+ SR) investigation of κ -(BEDT-TTF)₂Cu[N(CN)₂]Br. Our focus is the penetration depth in the vortex state for $T < T_c$ and the fluctuations of the local magnetic field in the normal state.

The layered structure of the κ -(BEDT-TTF)₂X family of organic molecular metals is shown in Fig. 1(a). The BEDT-TTF molecules dimerize, forming molecular units that stack on a triangular lattice in two-dimensional planes. The removal of one electron from each BEDT-TTF dimer causes the tight-binding band to be half filled, and to balance the charge, layers of anion X are located between the partially oxidized BEDT-TTF sheets. The properties of the system are strongly dependent on the transfer integral t , which is controlled by the dimer separation and may be manipulated by applying pressure or by changing the identity of the anion.² The phase diagram of the family [Fig. 1(b)] shows that the system may be tuned from Mott insulator through superconductivity into a normal metallic state as a function of t/U , where U is the onsite Coulomb repulsion (which is a property of the dimer and is almost independent of the anion or pressure). Importantly, this tuning is achieved without the need for chemical doping (in contrast to the cuprates) and therefore minimizes structural disorder effects. At small t/U , Coulomb correlations dominate and κ -(BEDT-TTF)₂X with $X = \text{Cu}[\text{N}(\text{CN})_2]\text{Cl}$ is a Mott insulator.⁸ As pressure is increased or X is changed to $X = \text{Cu}[\text{N}(\text{CN})_2]\text{Br}$, there is an insulator-to-superconductor transition.⁹ The $X = \text{Cu}(\text{NCS})_2$ compound is still further away from the Mott insulator phase and it remains a superconductor with a slightly depressed T_c .

Superconducting κ -(BEDT-TTF)₂Cu[N(CN)₂]Br ($T_c \approx 12$ K) displays several properties [Fig. 2] whose explanation remains obscure. These may be broadly grouped into three temperature regions. In region I ($T \approx 80$ K), there are sharp changes in the temperature dependence of the lattice constants⁷ [Fig. 2(d)] and, above 70 K, a rapid change in the thermal expansion coefficient perpendicular to the planes¹⁰ α_{\perp} [Fig. 2(e)]. These coincide with a rounded maximum in the resistivity¹¹ ρ [Fig. 2(b)]. The properties of this region have been linked to a glass-like freezing of terminal ethylene groups on the BEDT-TTF molecules¹⁰ around $T_g = 77$ K, although it has been suggested⁷ that this freezing alone cannot account for the observed structural changes. In region II ($T \approx 50$ K), NMR measurements^{2,12} yield a maximum in $1/T_1T$ around $T^* \approx 50$ K [Fig. 2(c)]. Upon cooling through this region, there is a crossover in transport properties from “bad metal” behavior to a more conventional Fermi-liquid regime,² and a plateau in α_{\perp} is also seen [Fig. 2(e)]. These phenomena have been linked to pseudogap physics, although the details remain unclear.² In region III ($T_c < T \lesssim 18$ K), a vortex Nernst signal is observed.⁶ It was argued⁶ that the proximity of the $X = \text{Cu}[\text{N}(\text{CN})_2]\text{Br}$ material to the Mott state in the phase diagram in Fig. 1(b) results in vortex fluctuations persisting above T_c and, furthermore, this remnant of fluctuating superconductivity may be consistent with the occurrence of phase fluctuations in the superconducting order parameter close to the Mott boundary.

This paper is structured as follows: after discussing experimental details in Sec. II, we present the results of transverse-field (TF) muon-spin relaxation measurements of the superconducting penetration depth of κ -(BEDT-TTF)₂Cu[N(CN)₂]Br in Sec. III. Section IV describes the use of longitudinal-field (LF) measurements to investigate spin fluctuations in the normal state of the material, and our conclusions are presented in Sec. V.

II. EXPERIMENTAL

Muon-spin spectroscopy¹³ is a sensitive means of probing the superconductivity and local magnetism of molecular

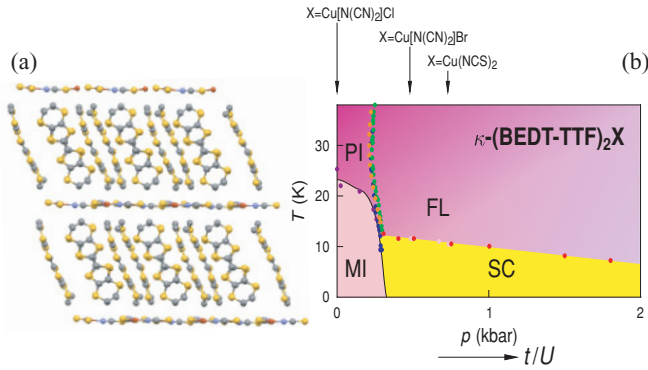


FIG. 1. (Color online) (a) Layered structure of the κ -(BEDT-TTF) $_2$ X system. (b) Phase diagram of the system showing the proximity of the $X = \text{Cu}[\text{N}(\text{CN})_2]\text{Br}$ salt to the Mott insulator phase (MI, Mott insulator; PI, paramagnetic insulator; SC, superconductor; and FL, Fermi liquid) (after Ref. 6).

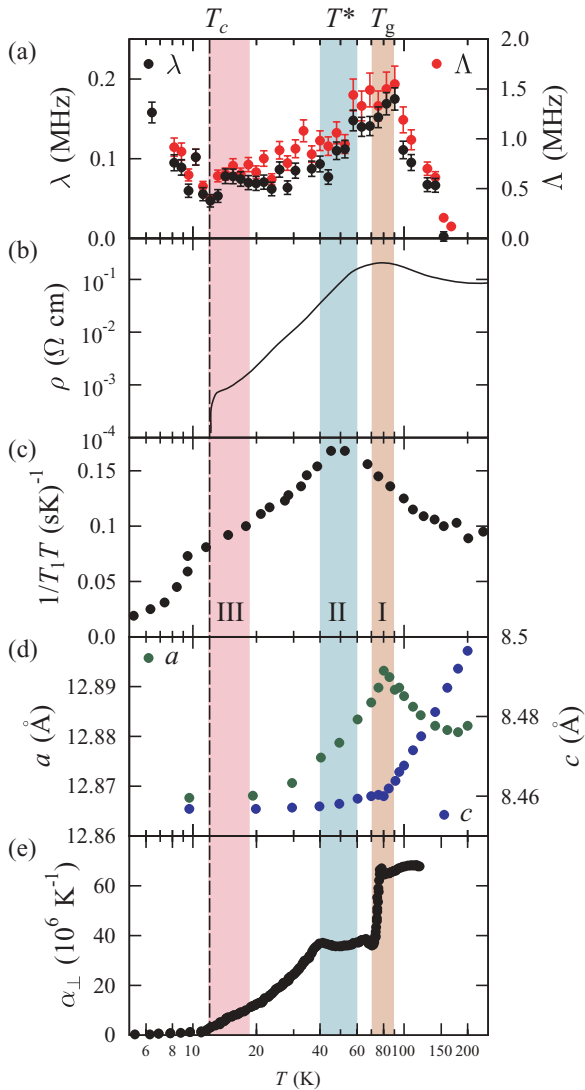


FIG. 2. (Color online) Comparison of several experimental properties with regions I ($T \approx 80$ K), II ($T \approx 50$ K), and III ($T_c < T \lesssim 18$ K) shaded. (a) LF μ^+ SR relaxation rates (this work), (b) resistivity,¹¹ (c) NMR $1/T_1T$,¹² (d) lattice constants,⁷ and (e) thermal expansion coefficient perpendicular to the layers.¹⁰

materials of this sort.^{14,15} TF and LF muon-spin relaxation (μ^+ SR) measurements were made on a mosaic sample of κ -(BEDT-TTF) $_2$ Cu[N(CN) $_2$ Br] at the ISIS facility, Rutherford Appleton Laboratory, United Kingdom, and the Swiss Muon Source (S μ S), Paul Scherrer Institut, Switzerland. The polycrystalline sample was made of ~ 50 small crystallites, which grow as platelets whose large faces are parallel to the conducting layers (the ac planes for this material). These were arranged on a piece of Ag foil to cover an area of ≈ 0.5 cm 2 so that the conducting layers are parallel to the plane of the mosaic. These measurements were made using a “fly-past” geometry¹⁶ to minimize background contribution from the sample holder. TF measurements were made using the MuSR spectrometer at ISIS, where the sample was mounted on a hematite backing plate in a helium cryostat with the sample oriented at 45° to both the applied magnetic field and the initial muon spin. To reduce any effect of ethylene disorder on the superconducting properties, the sample was slowly cooled at a rate of $\lesssim 5$ K/h. TF measurements were also made using the GPS instrument at S μ S, where the sample plane was oriented at 90° to the applied magnetic field and no slow-cooling procedure was followed. LF measurements were made on the ARGUS spectrometer (ISIS) in the latter 90° geometry without slow cooling.

III. TF μ^+ SR AND SUPERCONDUCTIVITY

TF μ^+ SR provides a means of accurately measuring the internal magnetic-field distribution in a material, such as that due to the vortex lattice (VL) in a type II superconductor.¹⁷ In a TF μ^+ SR experiment, spin-polarized muons are implanted in the bulk of a material in the presence of a magnetic field $B_{c1} < B_a < B_{c2}$, which is applied perpendicular to the initial muon spin direction. Muons stop at random positions on the length scale of the VL, where they precess about the total local magnetic field B at the muon site with frequency $\omega_\mu = \gamma_\mu B$, where $\gamma_\mu = 2\pi \times 135.5$ MHz T $^{-1}$. The observed property of the experiment is the time evolution of the muon-spin polarization $P_x(t)$, which allows the determination of the distribution $p(B)$ of local magnetic fields across the sample volume via $P_x(t) = \int_0^\infty p(B) \cos(\gamma_\mu Bt + \phi) dB$, where the phase ϕ results from the detector geometry.

Above T_c , some broadening of the spectrum is caused by randomly directed nuclear moments relaxing the muon spins. We also may have a small contribution from the fluctuations of electronic spins which we examine in detail in Sec. IV. Below T_c , the spectrum broadens considerably because of the contribution from the VL, but this component was found to be only $\sim 30\%$ of the total signal for $T < T_c$. Allowing for part of the nonsuperconducting signal to come from the cryostat and sample mounting material, we estimate that at most 50% of the sample is giving a superconducting signal. This is significant since it suggests that the majority of muons are not stopped in regions where there is a well-defined VL and may indicate the coexistence of a competing phase. In fact, there is good evidence for a phase separation between superconducting and insulating regions in this material,^{4,18} which is strongly dependent on disorder, such as that introduced through rapid cooling. While many of the previous indications of this effect have relied on surface sensitive experimental techniques, our

results appear to confirm the existence of phase separation throughout the bulk of the material. The nonsuperconducting contribution to our signal for $T < T_c$ decreases weakly and linearly with increasing temperature. Rapid cooling of the sample was found to reduce the superconducting volume fraction still further. With such a small superconducting fraction, it is difficult to accurately extract detailed line-shape information from our data. However, the root mean square (RMS) width of the VL field distribution B_{VL} can be straightforwardly obtained by fitting the data to the sum of two Gaussian relaxation components, reflecting the superconducting VL and nonsuperconducting contributions. These are easily separated below T_c since the contribution from the VL has a much larger relaxation rate, allowing us to consider the superconducting contribution alone. The field dependence of the VL component is shown in Fig. 3(a). The low-field data (40 mT and below) fit well to the width expected from the solution of a Ginzburg-Landau (GL) model of the triangular VL field distribution¹⁹ with an in-plane penetration depth of $0.47(1) \mu\text{m}$. B_{VL} is not very sensitive to B_{c2} in this field range, so we assume the reported value²² $B_{c2} = 10(2) \text{ T}$; the GL parameter κ is then estimated to be $80(10)$. The penetration depth in the highly conducting planes can also be estimated via the approximate expression for a high-anisotropy superconductor

$$\lambda_{\parallel} \approx (0.00371)^{\frac{1}{4}} \left(\frac{\Phi_0 \cos \theta}{B_{VL}} \right)^{\frac{1}{2}}, \quad (1)$$

where Φ_0 is the flux quantum and θ is the angle of the applied field with respect to the normal to the plane. This field-independent expression is valid at intermediate fields $B_{c1} \ll B_a \ll B_{c2}$, and the B_{VL} value obtained from Eq. (1) for $\lambda_{\parallel} = 0.47 \mu\text{m}$ is shown as the dashed line in Fig. 3(a); this is seen to be reasonably close to the field-dependent GL width in a field region centered around 10 mT.

Our value of λ_{\parallel} is smaller than previous reports, for example, the range $0.57 \leq \lambda_{\parallel} \leq 0.69 \mu\text{m}$ obtained from reversible high-field magnetization measurements,²³ and it is significantly lower than the value $\lambda_{\parallel} \approx 0.78 \mu\text{m}$ estimated from a previous μ^+ SR measurement²⁴ in a field of 300 mT. These differences can be understood by noting that the measured linewidth decreases sharply for $B_a \geq 80 \text{ mT}$ [Fig. 3(a)]. If this suppressed linewidth were taken to represent a full three-dimensional (3D) VL, a penetration depth of order $\lambda = 0.80 \mu\text{m}$ would also be obtained from our data using Eq. (1), in good agreement with the previous μ^+ SR result. The decrease in B_{VL} with applied field that we observe is not surprising, given the vortex phase diagram in (BEDT-TTF)₂Cu(NCS)₂.^{14,25} In that material the ideal 3D triangular VL that exists at low temperatures and low fields²⁶ is destroyed by the application of fields above a disorder-dependent threshold, which can be as low as 6 mT, causing a transition to a decoupled-layer vortex glass phase, accompanied by a sharp decrease in the measured linewidth.²⁵ It is therefore likely that a similar transition to a decoupled-layer vortex glass phase occurs in the $X = \text{Cu}[\text{N}(\text{CN})_2\text{Br}$ material above a threshold field in the 40- to 80-mT region. The effect on the width of the field distribution in the limit of losing all interlayer correlation has been calculated,^{27,28} giving

$$B_{2D}/B_{VL} = 1.4(s/a)^{1/2}, \quad (2)$$

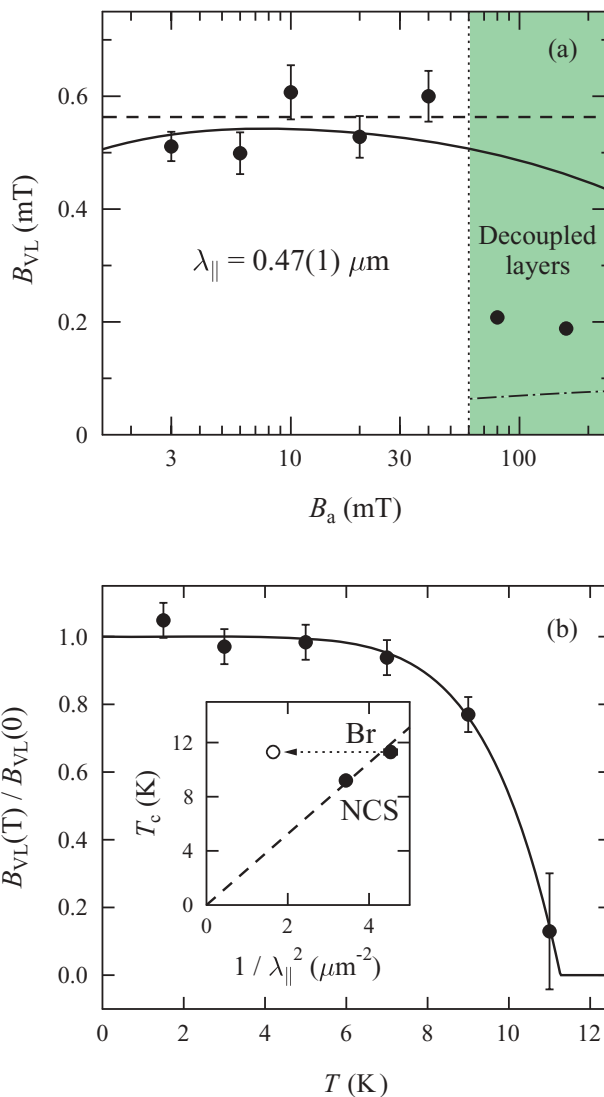


FIG. 3. (Color online) (a) Broadening of the 1.5-K TF μ^+ SR signal due to the VL measured at $S\mu\text{S}$. The field B_a was applied perpendicular to the conducting layers. The dotted line indicates a transition to a decoupled-layer vortex phase (shaded region) occurring between 40 and 80 mT. The solid line is the fit of the field-dependent line width¹⁹ below the vortex transition, giving $\lambda_{\parallel} = 0.47(1) \mu\text{m}$; the dashed line is the corresponding width predicted by Eq. (1). The dot-dash line shows the width according to Eq. (2) for fully decoupled vortex layers. (b) Temperature dependence of the normalised VL broadening measured at ISIS in the 3-mT field applied at 45° to the sample plane. A fit is shown to Eq. (3). The inset shows scaling between T_c and λ_{\parallel}^{-2} ,^{20,21} comparing the current data (Br) with that of κ -(BEDT-TTF)₂Cu(NCS)₂²¹; the open circle shifted to the left shows the apparent effect of applying $B_a \geq 80 \text{ mT}$ to Br.

where s is the interlayer spacing and a is vortex spacing within the layers. This limit is shown as the dot-dash line in Fig. 3(a), and it can be concluded that some residual interlayer correlations remain here since the data points are significantly above this limit. A further feature of our data in the decoupled vortex phase is that the superconducting fraction recovers to the larger value obtained in measurements made under slow-cooling conditions, suggesting that the disorder-induced phase

separation becomes significantly reduced once the layers are decoupled. In this picture, the cooling rate through T_g should be expected to determine the density of defects and hence the form of the pinning potential. The volume of superconducting regions is then determined by balancing the free energy savings introduced by the existence of superconductivity against the cost involved in the vortex lattice forming in a given pinning potential.²⁹

A previous study of the phase separation¹⁸ reveals that the characteristic size of the phase-separated regions is 50–100 μm . This is very large compared to the penetration depth and the length scale over which we would expect a single muon to be sensitive, and so we would not expect a significant contribution to our measurement of B_{VL} (and the resulting penetration depth) from effects related to the phase separation such as distortion of the VL near domain walls. The temperature dependence of B_{VL} has been measured in a field of 3 mT applied in a 45° geometry, and this is shown in Fig. 3(b). This can be fitted to an empirical power law

$$B_{\text{VL}}(T) = B_{\text{VL}}(0)[1 - (T/T_c)^r], \quad (3)$$

where $B_{\text{VL}}(0)$ is the zero-temperature contribution from the VL. Therefore, the VL here appears to thermally stable, in contrast to the case of $(\text{BEDT-TTF})_2\text{Cu}(\text{NCS})_2$, where a clear melting of the VL is seen.³⁰ The values $B_{\text{VL}}(0) = 0.31(1)$ mT and $T_c = 11.3(4)$ K are obtained from the fit. The penetration depth in the highly conducting planes could be obtained by taking $\theta = 45^\circ$ in Eq. (1); however, the absolute accuracy is reduced compared to 90° measurements for two reasons: first, the width measured at 45° is particularly sensitive to any angular misalignment between the sample and field, and second, the angular scaling in highly anisotropic superconductors can be much more complex than the simple form implied by Eq. (1).³¹ Returning to the 90° data, we note that a marginally better fit is obtained by allowing for an asymmetric lineshape¹⁴ parametrized using the skewness parameter $\beta = (\langle B \rangle - B_a)/B_{\text{VL}}$. The optimum fit is achieved with $\beta = 0.7$, which is reasonably close to the ideal triangular lattice value of 0.60 that was observed in more detailed studies of the vortex phases of the $X = \text{Cu}(\text{NCS})_2$ compound.²⁵ This fit also yields $0.47(1)$ μm for λ_{\parallel} . The values obtained here and in previous muon studies for 90° geometry are summarized in Table I. We may compare our values of λ_{\parallel} and T_c for the $X = \text{Cu}[\text{N}(\text{CN})_2]\text{Br}$ material to values obtained previously for the $X = \text{Cu}(\text{NCS})_2$ material. This is shown as the inset to Fig. 3(b) and suggests that there is a scaling relation between these two parameters. Although this pair of κ -phase

points are rather close, a scaling relation²⁰ $T_c \propto \lambda^{-2}$ would be reasonably consistent with the data. More generally, applying a $T_c \propto \lambda^{-3}$ scaling has been suggested when a broader range of molecular superconductors is considered,²¹ but more data would be required to test whether this holds within the subset of κ -phase BEDT-TTF compounds.

IV. LF μ^+ SR AND SPIN FLUCTUATIONS

We now turn to the local magnetic fluctuations in the normal state of this system, which we probe with LF μ^+ SR measurements made in a field of $B = 2$ mT (after fast cooling). In these measurements, the initial muon spin is directed parallel to the applied field, and we measure the polarization $P_z(t)$ along the same direction via the muon asymmetry function $A(t) [\propto P_z(t)]$. Dynamics in the local magnetic field distribution will cause muon spins to flip, leading to a depolarization with relaxation rate Λ . The small applied longitudinal field was intended to quench the contribution to the spectra of background from nuclear moments, allowing the contribution due to electron-spin dynamics to be discerned. In a previous muon study of a related BEDT-TTF material,¹⁵ muons were shown to be sensitive to magnetic order within the organic layers, but only a small relaxing asymmetry was observed. We therefore expect that our results will reflect magnetic fluctuations within the organic layers of κ -(BEDT-TTF) $_2X$.

A typical LF μ^+ SR spectrum measured at 20 K is shown in Fig. 4(a). Above 100 K, our spectra are best described with a single exponential function with relaxation rate Λ characteristic of dynamic fluctuations in the local magnetic field at the muon sites in the material. For $T < 100$ K, there is a single, highly damped, temperature-dependent oscillation visible for times $t \leq 4$ μs . In this context, spectra of this form suggest a contribution from quasistatic disordered magnetic moments, which are typically described by a Kubo-Toyabe (KT) function³³ $f_{\text{KT}}(\Delta, B, t)$. Our data are best fitted using this function with a constant field width $\Delta = 0.72$ MHz for all $T < 100$ K and modeling the dynamic contribution to the spectra for $T < 100$ K by multiplying by an exponential factor $e^{-\Lambda t}$. The data were fitted to the resulting functional form

$$A(t) = A_0 f_{\text{KT}}(\Delta, B, t) e^{-\Lambda t} + A_{\text{bg}}. \quad (4)$$

The extracted relaxation rates Λ are shown in Figs. 2(a) and 4(b). Other parametrizations are possible but lead to less successful fits. However, for comparison, a fit across the measured temperature regime of a single exponential with relaxation rate Λ is shown in Fig. 2(a), where we see that both track the same behavior. For comparison with the NMR $1/T_1 T$ results, we also show Λ/T in Fig. 4(c). The most dramatic feature of the data is the large maximum in Λ , which occurs around $T = 100$ K. The sharp decrease in relaxation rate above around 100 K broadly coincides with region I, which may suggest a link with the ethylene disorder effects and glasslike transition in this region. Given the crossover in behavior of the system near region I observed with several other experimental probes [Fig. 2(b)], one explanation is that above 100 K there is a change in the nature of the muons' coupling to the material and that at these elevated temperatures a different relaxation channel opens up.

TABLE I. Comparison of penetration depth λ_{\parallel} extracted from μ^+ SR measurements under different experimental conditions.

Anion	Study	Skewness	B_a (mT)	λ_{\parallel} (μm)
Cu[N(CN) $_2$ Br	This study	0	3–40	0.47(1)
Cu[N(CN) $_2$ Br	This study	0.7	3	0.47(1)
Cu[N(CN) $_2$ Br	This study	0	160	0.82(1)
Cu[N(CN) $_2$ Br	Ref. 24	0	300	0.78
Cu(NCS) $_2$	Ref. 14	0.38	2.5	0.54(2)
Cu(NCS) $_2$	Ref. 32	0	13–400	0.77(7)

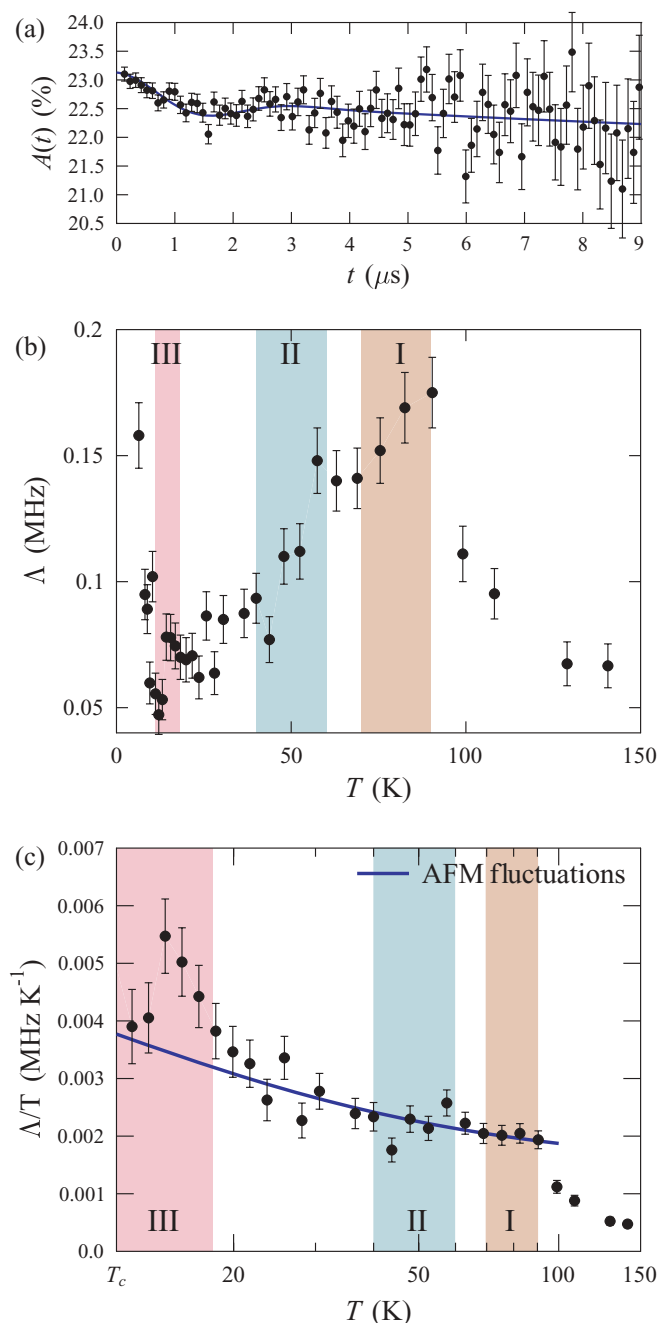


FIG. 4. (Color online) (a) Typical spectra measured in a LF of $B = 2$ mT at $T = 20$ K. (b) Evolution of Δ with T extracted from fits to Eq. (4). Regions I, II, and III are shaded. (c) Temperature evolution of Δ/T . A fit to a model of antiferromagnetic spin fluctuations is shown.

When compared to the results of Ref. 15, the relaxing amplitude we observe appears very small, leading us to believe that the relaxation arises from only a fraction of the muon sites in the material. Since, in our material, we expect phase separation into (i) metallic regions that turn superconducting on cooling through T_c and (ii) insulating regions that do not superconduct, we would expect the μ^+ SR to reflect this. It is therefore likely that the observed relaxation arises from only one of the phases.

We first consider the possibility that the relaxation results from electronic fluctuations within insulating regions of the sample. By analogy with the $X = \text{Cu}[\text{N}(\text{CN})_2]\text{Cl}$ material, we might expect these regions to be paramagnetic at elevated temperatures with a possibility of antiferromagnetic order at a reduced temperature. We note that the fitted value of Δ above is quite large for randomized nuclear fields (where typically $\Delta < 0.3$ MHz) and given the small size of the electronic moments observed with muons in BEDT-TTF layers previously,¹⁵ it may be that this signal results from a population of quasistatic, disordered magnetic moments. However, there is no smooth decrease in Δ with increasing T as would occur in the presence of magnetic order. We note also that we do not observe a large increase in Δ as T is reduced, as one would expect for a paramagnetic material as a transition is approached from above.

The alternative interpretation is that the relaxation arises from the metallic regions of the material. At temperatures $T < 100$ K, the dominant trend is a roughly linear increase in relaxation rate with T up to around 100 K. The linear regime observed for $T < 100$ K may be indicative of Korringa law relaxation,³⁴ resulting from flip-flop transitions of electronic and muon spins, and is expected to lead to a relaxation rate $\Lambda = \frac{1}{T_1} \propto k_B T \sum_{\mathbf{q}} A(\mathbf{q})^2 \lim_{\omega \rightarrow 0} \chi''(\mathbf{q}, \omega)/\omega$, where $\chi''(\mathbf{q}, \omega)$ is the imaginary part of the dynamic magnetic susceptibility and $A(\mathbf{q})$ is the hyperfine coupling. For the case of a \mathbf{q} -independent coupling, we obtain $\lambda \propto k_B T [A\chi(0,0)]^2$, showing that the muon relaxation rate would probe the local spin susceptibility $\chi(\mathbf{q} = 0, \omega = 0)$ for relaxation of this sort.

To further investigate the temperature evolution of the local susceptibility from Korringa relaxation, we may consider $\Lambda/T (\equiv 1/T_1 T)$ against T in Fig. 4(c). We see that on warming above T_c the quantity Λ/T peaks at around 15 K before decreasing sharply around region III ($15 < T \lesssim 25$ K), indicating a significant decrease of the local magnetic susceptibility in this region. Above 30 K, Λ/T decreases only gradually throughout region II, dropping off suddenly in region I. These muon Λ/T results are quite different than the NMR $1/T_1 T$ results for this material (Fig. 2), where a larger peak is seen in region II. We do not see any dramatic change of behavior in region II in the μ^+ SR results, and there is no suggestion of any anomaly in the NMR behavior in regions I and III. In fact, the NMR results for $50 \text{ K} < T < 300 \text{ K}$ are well described by a model of antiferromagnetic spin fluctuations⁵ based on the Millis-Monien-Pines model,³⁵ which predicts $1/T_1 T \approx A + B/(T/T_x + 1)$, where A and B are constants that depend on the correlation length of the spin fluctuations whose energy scale is determined by the temperature parameter T_x . As shown Fig. 4(b), the model does not fit the muon Λ very well for $T < 100$ K and becomes gradually worse as region III is approached from above. However, given that the muon sites in this material are likely to be different than the ^{13}C site where the nuclear resonance is achieved,¹² it is possible that the muon will probe a quite different field distribution than that probed in NMR. We note further that our muon results are also quite different than the LF μ^+ SR behavior observed in molecular superconductors such as the alkali-fullerides,³⁶ where Λ/T is quite featureless above T_c .

In view of these considerations, it is difficult to provide a conclusive explanation for the unusual form of the relaxation

that we have observed in the region $T_c < T < 100$ K. It would be desirable in the future to extend μ^+ SR studies of the normal-state magnetic properties to the other members of this series to follow how these features evolve across the phase diagram.

V. CONCLUSIONS

In conclusion, our investigation of the superconducting and normal-state properties of κ -(BEDT-TTF)₂Cu[N(CN)₂]Br using implanted muons has allowed us to identify a number of experimental features of this system. In the superconducting phase, two important effects are seen: first, a reduced superconducting signal fraction that is affected by sample cooling rate and is consistent with the phase separation suggested by earlier studies, and second, a vortex transition taking place between 40 and 80 mT that reduces the width of the magnetic-field distribution for higher measurement fields. By taking these two effects carefully into account, we have obtained an improved and more reliable estimate for the $T = 0$ in-plane penetration depth $\lambda_{\parallel} = 0.47(1)$ μm and find that the

trend of T_c increasing with superfluid stiffness $\rho_s \propto 1/\lambda_{\parallel}^2$ for κ -(BEDT-TTF)₂X superconductors is consistent with the overall trend for molecular superconductors, whereas previous data had suggested that κ -(BEDT-TTF)₂Cu[N(CN)₂]Br was anomalous in this regard. In the normal state, we find a large peak in the longitudinal muon spin relaxation rate around 100 K, coinciding with the region where ethylene disorder effects are prevalent.

ACKNOWLEDGMENTS

We are grateful to Alex Amato, Andrew Steele, and Peter Baker for experimental assistance and to EPSRC (United Kingdom) for financial support. Part of this work was performed at S μ S and part at the STFC ISIS facility, and we are grateful to PSI and STFC for the provision of beamtime. Work was supported by U. Chicago Argonne, LLC, operator of Argonne National Laboratory. Argonne, a US Department of Energy Office of Science laboratory, is operated under Contract No. DE-AC02-06CH11357.

*t.lancaster1@physics.ox.ac.uk

¹T. Ishiguro, K. Yamaji, and G. Saito, *Organic Superconductors*, 2nd ed. (Springer, Berlin, 2006).

²B. J. Powell and R. H. McKenzie, *J. Phys. Condens. Matter* **18**, R827 (2006).

³K. Sano, T. Sasaki, N. Yoneyama, and N. Kobayashi, *Phys. Rev. Lett.* **104**, 217003 (2010).

⁴O. J. Taylor, A. Carrington, and J. A. Schlueter, *Phys. Rev. B* **77**, 060503(R) (2008).

⁵E. Yusuf, B. J. Powell, and R. H. McKenzie, *Phys. Rev. B* **75**, 214515 (2007).

⁶M.-S. Nam, A. Ardavan, S. J. Blundell, and J. A. Schlueter, *Nature (London)* **449**, 584 (2007).

⁷A. U. B. Wolter, R. Feyherherm, E. Dudzik, S. Süllow, C. Strack, M. Lang, and D. Schweitzer, *Phys. Rev. B* **75**, 104512 (2007).

⁸F. Kagawa, M. Miyagawa, and K. Kanoda, *Nature (London)* **436**, 534 (2005).

⁹J. M. Williams *et al.*, *Inorg. Chem.* **29**, 3272 (1990).

¹⁰J. Müller, M. Lang, F. Steglich, J. A. Schlueter, A. M. Kini, and T. Sasaki, *Phys. Rev. B* **65**, 144521 (2002).

¹¹R. C. Yu, J. M. Williams, H. H. Wang, J. E. Thompson, A. M. Kini, K. D. Carlson, J. Ren, M.-H. Whangbo, and P. M. Chaikin, *Phys. Rev. B* **44**, 6932 (1991).

¹²K. Miyagawa, K. Kanoda, and A. Kawamoto, *Chem. Rev.* **104**, 5635 (2004).

¹³S. J. Blundell, *Contemp. Phys.* **40**, 175 (1999).

¹⁴S. L. Lee, F. L. Pratt, S. J. Blundell, C. M. Aegerter, P. A. Pattenden, K. H. Chow, E. M. Forgan, T. Sasaki, W. Hayes, and H. Keller, *Phys. Rev. Lett.* **79**, 1563 (1997).

¹⁵K. Satoh, H. Taniguchi, A. Kawamoto, and W. Higemoto, *Physica B* **374–375**, 99 (2006).

¹⁶M. C. Lynch, S. P. Cottrell, P. J. C. King, and G. H. Eaton, *Physica B* **326**, 270 (2003).

¹⁷J. E. Sonier, J. H. Brewer, and R. F. Kiefl, *Rev. Mod. Phys.* **72**, 769 (2000).

¹⁸N. Yoneyama, T. Sasaki, N. Kobayashi, Y. Ikemoto, and H. Kimura, *Phys. Rev. B* **72**, 214519 (2005).

¹⁹E. H. Brandt, *Phys. Rev. B* **68**, 054506 (2003).

²⁰Y. J. Uemura *et al.*, *Phys. Rev. Lett.* **62**, 2317 (1989); Y. J. Uemura *et al.*, *ibid.* **66**, 2665 (1991).

²¹F. L. Pratt and S. J. Blundell, *Phys. Rev. Lett.* **94**, 097006 (2005).

²²H. Elsinger, J. Wosnitza, S. Wanka, J. Hagel, D. Schweitzer, and W. Strunz, *Phys. Rev. Lett.* **84**, 6098 (2000).

²³N. Yoneyama, A. Higashihara, T. Sasaki, T. Nojima, and N. Kobayashi, *J. Phys. Soc. Jpn.* **73**, 1290 (2004).

²⁴L. P. Le, G. M. Luke, B. J. Sternlieb, W. D. Wu, Y. J. Uemura, J. H. Brewer, T. M. Riseman, C. E. Stronach, G. Saito, H. Yamochi, H. H. Wang, A. M. Kini, K. D. Carlson, and J. M. Williams, *Phys. Rev. Lett.* **68**, 1923 (1992).

²⁵F. L. Pratt, S. L. Lee, C. M. Aegerter, C. Ager, S. H. Lloyd, S. J. Blundell, F. Y. Ogrin, E. M. Forgan, H. Keller, W. Hayes, T. Sasaki, N. Toyota, and S. Endo, *Synth. Met.* **120**, 1015 (2001).

²⁶L. Ya. Vinnikov, T. L. Barkov, M. V. Kartsovnik, and N. D. Kushch, *Phys. Rev. B* **61**, 14358 (2000).

²⁷D. R. Harshman, E. H. Brandt, A. T. Fiory, M. Inui, D. B. Mitzi, L. F. Schneemeyer, and J. V. Waszczak, *Phys. Rev. B* **47**, 2905 (1993).

²⁸E. H. Brandt, *Rep. Prog. Phys.* **58**, 1465 (1995).

²⁹G. Blatter, M. V. Feigel'man, V. B. Geshkenbein, A. I. Larkin, and V. M. Vinokur, *Rev. Mod. Phys.* **66**, 1125 (1994).

³⁰F. L. Pratt, S. J. Blundell, T. Lancaster, M. L. Brooks, S. L. Lee, N. Toyota, and T. Sasaki, *Synth. Met.* **152**, 417 (2005).

³¹F. L. Pratt, I. M. Marshall, S. J. Blundell, A. Drew, S. L. Lee, F. Y. Ogrin, N. Toyota, and I. Watanabe, *Physica B* **326**, 374 (2003).

³²D. R. Harshman, A. T. Fiory, R. C. Haddon, M. L. Kaplan, T. Pfiz, E. Koster, I. Shinkoda, and D. L. Williams, *Phys. Rev. B* **49**, 12990 (1994).

³³R. S. Hayano, Y. J. Uemura, J. Imazato, N. Nishida, T. Yamazaki, and R. Kubo, *Phys. Rev. B* **20**, 850 (1979).

³⁴S. J. Blundell and S. F. J. Cox, *J. Phys. Condens. Matter* **13**, 2163 (2001).

³⁵A. J. Millis, H. Monien, and D. Pines, *Phys. Rev. B* **42**, 167 (1990).

³⁶W. A. MacFarlane, R. F. Kiefl, S. Dunsiger, J. E. Sonier, J. Chakhalian, J. E. Fischer, T. Yildirim, and K. H. Chow, *Phys. Rev. B* **58**, 1004 (1998).